Post-print of: Wilde K., Bruski D., Budzyński M., Burzyński S., Chróścielewski J., Jamroz K., Pachocki Ł., Witkowski W.: Numerical Analysis of TB32 Crash Tests for 4-cable Guardrail Barrier System Installed on the Horizontal Convex Curves of Road. INTERNATIONAL JOURNAL OF NONLINEAR SCIENCES AND NUMERICAL SIMULATION. DOI: 10.1515/ijnsns-2018-0169

Numerical analysis of TB32 crash tests for 4-cable guardrail barrier system installed on the horizontal convex curves of road

Krzysztof Wilde[1], *Dawid* Bruski[1,*], *Marcin* Budzyński[2], *Stanisław* Burzyński[1], *Jacek* Chróścielewski[1], *Kazimierz* Jamroz[2], *Łukasz* Pachocki[1] and *Wojciech* Witkowski[1]

[1]Gdańsk University of Technology, Faculty of Civil and Environmental Engineering, Department of Mechanics of Materials and Structures, ul. Gabriela Narutowicza 11/12, 80-233 Gdańsk, Poland
[2]Gdańsk University of Technology, Faculty of Civil and Environmental Engineering, Highway and Transportation Engineering Department, ul. Gabriela Narutowicza 11/12, 80-233 Gdańsk, Poland

Abstract. Horizontal curves are one of the elements of road infrastructure where statistically a relatively high number of accidents have been reported. In the last ten years in Poland approx. 10% of all road accidents happened on horizontal curves of roads and was responsible for approx. 14% of all fatalities on Polish roads. Thus, this issue is important and requires extensive research and proper road safety treatments. One possible measure that may contribute to improvement of safety on road curves may be barriers. The purpose of this work is to assess, with use of numerical simulations, the performance of the 4-cable barrier systems installed on horizontal road convex curves. The most important parameters for road safety barriers are presented including the effect of various impact velocities and the radiuses of the road curves.

Keywords: road safety equipment, numerical simulations, crash tests, road curves, Finite Element Method, LS-DYNA

1 Introduction

1.1 OUTLINE OF THE PROBLEM

The contemporary approach to safety distinguishes three integrated elements: infrastructure measures, safety management and safety culture [21], [37]. Because of its complexity, the process of safety management needs modern tools to help identify road user risks, estimate and assess road infrastructure safety and select effective safety treatments. The selection of safety measures must be preceded with an understanding of the effects of selected factors on road safety at different levels of management.

Road infrastructure and roadsides can be a factor causing road accidents when road user errors occur (e.g. elements that are not easily comprehended or clear, poorly organised traffic, curbed visibility, geometric parameters not adequate for the speeds) and have a strong influence on accident severity, especially where accidents are concerned [12], [17], [35]. Run-off-road accidents and their consequences can be reduced by improving the road and street network, completing and reconstructing the existing network, developing and implementing "self-explanatory roads", developing and implementing "forgiving roads" and providing road signs and markings that are more understandable and road user friendly. One of the devices supporting these actions is the use of road safety barriers. Before appropriate steps are taken, it is necessary to recognise the conditions in which hazards on the road occur and the effectiveness of the equipment used. These accidents represent app. 19% of all of Poland's road deaths. Roadside crashes involve (based on SEWIK, a police database): hitting a tree (the main hazard), hitting a barrier, hitting a sign or utility pole, vehicle roll-over on the roadside, vehicle roll-over on a slope and vehicle roll-over into a ditch. The main consequence of a roadside hazard is not the likelihood of an accident itself but of its severity [1], [34]. Safety barriers are also part of the roadside. While they protect motorists from hitting an obstacle or stop vehicles from leaving the road in the case of steep embankments, they are obstacles themselves, which if poorly designed and built, may pose a serious risk [29], [68].

Vehicles are more likely to leave the carriageway on horizontal curves due to the forces that are subjected to. With an estimated 40% of people killed in run-off-road accidents occurring on and around horizontal curves, it is clear how serious the problem is, i.e. a combination of horizontal curves with hazardous roadsides.

This calls for a special analysis of horizontal curves for their accident risk with a focus on evaluating roadsides on and around curves (presence of obstacles, shoulders and embankments, safety barriers). Fig. 1 shows examples of roadside hazards on horizontal curves.

Fig. 1 Examples of roadside hazards on horizontal curves.

The design of safety measure models including a road's vertical alignment uses a number of variables:

- a division into straight sections and sections with curves [20],
- length of straight road sections [14],
- density of horizontal curves/length of curve per kilometre of road/presence of curves with big turning angles [31],
- route turning angle [23],
- density/number of vertical curves [38],
- occurrence of transition curve [22],
- radius/length of horizontal curve [30],
- road curvature [2], [32], [15].

Because the necessary data are difficult to obtain, Poland's road safety measure models do not include horizontal curve parameters. While the variables in many of the models include road geometry parameters, it is not clear how they affect road safety [36]. Given Poland's very high share of run-off-road fatalities, horizontal curve parameters are particularly important. With an estimated 40% of people killed in run-off-road accidents occurring on and around horizontal curves, it is clear how serious the problem is, i.e. a combination of horizontal curves with hazardous roadsides. Horizontal curves and their parameters have a strong effect on road safety [33] [41] [46] [47]. Horizontal curves are strongly correlated to speed and visibility [16] [67]. The characteristics of speed profiles and the profile and curvature of vehicle trajectory on curves in vertical alignment are affected by the road's qualitative features such as radius, turning angle, width of roadway and roadway conditions caused by the weather (dry and wet conditions) [11]. Visibility is curbed when horizontal curve areas include junctions, elements of interchanges (ramps), pedestrian crossings, etc. There may be additional hazards when demand for overtaking and speed dispersion are high. In conditions of limited visibility, head-on collisions are a real risk.

Because run-off-road accidents are a frequent occurrence on horizontal curves, it is important to use the right road safety equipment, especially safety barriers, by looking at the location, type (containment level, working width) and kind (cable, steel, concrete). Fig. 2 shows examples of road accidents on horizontal curves as a result of hitting a barrier.

Fig. 2 Examples of accidents – hitting a barrier on horizontal curves (source: GDDKiA)

In Poland between 2007 and 2016 there were 46,800 accidents on horizontal curves representing about 15% of all accidents in Poland. The accidents involved 65,900 injuries (13% of all injuries) and 6,400 people killed (16% of all fatalities). In 2016 there were nearly 4,000 accidents on curves (12% of all accidents) involving more than 5,000 injuries (13% of all injuries) and more than 500 people killed (15% of all fatalities). The data show that safety on horizontal curves is a serious problem and that efforts must be taken to improve road user safety.

Analysis of the types of accidents on horizontal curves (2012 – 2016) showed that roadside-related accidents represent 29% of all accidents on curves and involve 27% of all injuries on curves and 38% of all fatalities which occur on this element of road infrastructure. The details are presented in Table 1 and Fig. 3. Roadside accidents and their casualties are highlighted.

Horizontal curve accidents involving the roadside only include primarily hitting a tree – 54% of accidents and 72% of fatalities and vehicle roll-over off the road (shoulder, ditch, embankment) - 20% of accident and 11% fatalities.

The share of accidents involving hitting a safety barrier on horizontal curves represents 3% of all accidents on curves. As regards injuries and fatalities, they account for 3% of all injuries and fatalities respectively. This is not to say that safety barriers on horizontal curves do not represent a safety issue. Instead the data show that too few sections with horizontal curves have safety barriers. The severity of run-off-road accidents on horizontal curves and hitting a tree – 22 fatalities per 100 accidents - compared to the severity of accidents involving hitting a safety barrier (11 fatalities per 100 accidents) confirms how critical it is to secure this element of the road network

Table 1 Types of road accidents on horizontal curves 2012-2016

Type of road incident	accidents	injuries	serious injuries	fatalities
Other	2247	2961	761	126
Hitting a safety barrier *	642	808	199	72
Hitting a tree *	3176	4040	1409	712
Hitting a pedestrian	1548	1476	555	251
Hitting a pole, sign *	864	1080	306	99
Vehicle roll-over on the road	3229	4057	1013	240
Vehicle roll-over on the roadside *	1169	1538	455	112
Vehicle side crash	2625	3530	916	282
Vehicle head-on collision	4276	7474	2283	669
Vehicle rear crash	708	924	179	60
Total	**20484**	**27888**	**8076**	**2623**

* roadside accidents

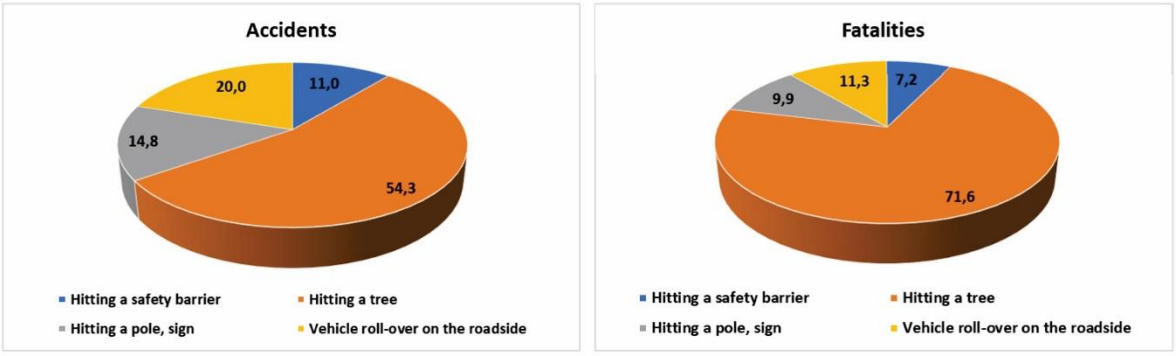

Fig. 3 Percentage of accidents and fatalities on horizontal curves involving the roadside

Given the high frequency of run-off-road accidents on horizontal curves, it is important to ensure that the right road safety equipment is used, in particular safety barriers, with the right location, type (level of containment, working width) and construction (wire rope, steel, concrete).

When selecting vehicle restraints and their location, it is important to use supporting tools such as site tests and numerical tests. Numerical tests help to complement data obtained from field tests. Because selected parameters can be modified (angle of impact, speed of impact), it is possible to identify optimal solutions for the specific road and traffic conditions. When conducting tests of barriers on horizontal curves an additional parameter can be added, i.e. curve radius.

Table 2 gives a range of possible horizontal curve radii and the potential speeds of impact based on "Technical conditions for roads" [60]. The values highlighted refer to the consequences of exceeding speed limits. However, it needs to be stressed that driving above the speed limit is a very frequent occurrence in Poland. In addition, please note that as speed increases and horizontal curve radii decrease, the lateral inclination increases on the curve which changes the impact of forces a vehicle on a curve is subjected to when hitting a barrier. The tests below did not include this.

Table 2 Range of horizontal curve radii for potential speeds of hitting a barrier.

V [km/h]/R [m]	Straight	900	600	400	200	100
140 km/h						
110 km/h						
90 km/h						
70 km/h						
50 km/h						

Parameters resulting from public road technical conditions [60]
Cases of exceeding speed limits

Designed to stop errant vehicles from leaving the road, road and bridge safety barriers are mounted in sites where the risk of serious injury and fatality is higher if they are not provided. Safety barriers can be divided into concrete, steel and cable barriers. Cable barriers are a frequently used road safety device in Poland. Installed on express roads (e.g. about 60 km of barriers on the A1 motorway) and general roads, safety barriers can be mostly found on central reservations and on the edge of the road. Cable barriers are flexible systems comprising of three or four tensioned wire ropes, supported by posts and ground anchors. They are more flexible than other barrier types, resulting in minimised vehicle damage and occupant injury. Tension in the cables is what allows cable barriers to redirect vehicles. Cable barriers are generally perceived as a beneficial structure and they usually provide smaller decelerations for vehicle's occupants during impact than other types of barriers. Also the number of road accidents with low severity, where passengers are not seriously injured and the vehicle after impact can often continue to drive, is higher than in the case of steel or concrete barriers [42] [43]. The posts in the cable barrier are designed so that they can be easily bent to the ground surface and enable the longitudinal structural elements (cables) to absorb the energy from the vehicle impact through elongation (stretching). These effects cause the barrier to deflect laterally in a parabolic form that assists in redirecting the vehicle back on the travel lane in a smooth manner [25]. However, it is emphasized here, that cable barriers are not universal devices and in some cases on road there might be a need to use other types of barriers with different properties. Once installed, the system should be analysed for its performance on horizontal curves due to the specificity of the design. Horizontal curves affect cable barrier performance and must be considered when deciding where to place the cable barriers. To that end the effects of the horizontal curve on the performance of the system should be studied for different velocities of cable barrier impact. According to the report [25], impacts on the concave side of a curved cable barrier are not a problem but impacts on the convex side might result in significantly higher deflections because of the slackening of the wire ropes that can take place. For this reason, this research has been aimed to analyse only the impacts on the convex side of the curved cable barrier.

1.2 Testing of safety barrier systems

Nowadays, based on [24], each barrier installed on the road in Poland must be tested in accordance with EN 1317 Standards [48] [49]. The standard describes three basic functional characteristics of the safety barrier: containment level, working width and impact severity level, which are obtained from full-scale crash tests. It is highlighted here that the EN1317 standards do not specify conditions for barrier's geometry, dimensions and materials. Containment levels describe the barrier's ability to contain impacting vehicle for various types of vehicles, various impact velocities and angles. EN 1317 standard distinguishes four containment level: low angle containment, normal containment, higher containment and very high containment. The working width describes barrier's deformation during vehicle's impact and is defined as the maximum lateral distance between any part of the barrier on the undeformed traffic side and the maximum dynamic position of any part of the barrier or vehicle. This value informs about the distance behind the barrier, which should be free from obstacles to enable correct performance of the restraint system. Impact severity level is a measure of impact effects on the vehicle occupants. To determine this level two indicators are needed: the acceleration severity index (ASI) and the theoretical head impact velocity (THIV). ASI allows for assessment of the injuries of occupants during impact and is one of the most important parameters which. ASI is computed using the following formula:

$$\mathrm{ASI}(t) = \sqrt{\left(\frac{\bar{A}_x}{\hat{a}_x}\right)^2 + \left(\frac{\bar{A}_y}{\hat{a}_y}\right)^2 + \left(\frac{\bar{A}_z}{\hat{a}_z}\right)^2} \tag{1}$$

where $\bar{A}_x$, $\bar{A}_y$, $\bar{A}_z$ are the acceleration along the body axes x, y and z at the vehicle's centre of gravity which are filtered with a four-pole phaseless Butterworth low-pass digital filter with the cut-off frequency of 13 Hz, $\hat{a}_x$ = 12 g, $\hat{a}_y$ = 9 g, $\hat{a}_z$ = 10 g are limit values for the acceleration components. As a measure of severity level the maximum value of the ASI during impact is assumed. THIV index is an velocity at which the theoretical head hits the theoretical surfaces within the interior of the vehicle during collision. It is assumed that the initial velocity of the theoretical head at the beginning of the impact is equal to the velocity of vehicle. Then, due to the hitting a road restraint system the vehicle rotates about its vertical axis, however the theoretical head still move in a straight line. The value of THIV index is the head's velocity at the moment of impact with theoretical surface. The values: ASI ≤ 1 and THIV ≤ 33 km/h ensure the highest level of safety – level A.

EN 1317 Standards [48] [49] consider only straight sections of barriers. However, in reality many different situations may occur i.e. barriers installed on horizontal and vertical road curves [13], [65], various impact velocities [44], and angles [9], various types of vehicles or different barrier lengths, in particular the length of the barrier may be shorter than the length of the barrier tested according the standards and because of this may not be as secure as their full-length parent [63]. The multitude of potential scenarios that can happen on the road gives the rise to application of numerical simulations. They are commonly used to study the performance of safety barriers in parallel with full-scale crash tests. Moreover, part 5 of the EN1317 standards [50] enables the use numerical simulations to certify under certain conditions system of safety barrier which was modified. In recent years, a significant increase of using numerical simulations in the context of road safety research has been observed. In 2012 the standards describing guidelines for numerical simulation of crash test and requirements regarding correct verification of the model and validation process of the virtual crash test have been published [51] [52] [53] [54]. Therefore, a number of works in which the results of crash test simulations have been presented, e.g. [8], [10], [18], [26], [27], [64]. Among many publications the most valuable ones are those supported by the results of the full scale crash test, e.g. [40], [61], [62]. These publications confirm the usefulness of numerical simulations for testing the safety properties of road restraint systems.

2 Numerical model

2.1 LS-DYNA system

LS-DYNA is a well-known and widely used commercial FEM code, designed to deal with highly nonlinear, short lasting phenomena. In the present research, explicit dynamics solver is used, due to its robustness in solving problems with very large number of degrees of freedom, many material laws included and possible complex contact behaviour. Another advantage of LS-DYNA is its parallelization, what makes calculations scalable up to hundreds of computer cores. Nevertheless, an explicit dynamics algorithm is conditionally stable. It means that the time step, in calculations, should be very small and it is dependent, among others, on the characteristic size of the finite element. Furthermore, the time step size must be compromise between the total calculation time and the level of details in the model.

In a typical LS-DYNA model, beside geometrical data, dozens of materials definitions are included, with hundreds of parameters defined. Some of them ale collected from laboratory tests, some of them are proposed in scientific journals, some of them are defined according to common engineering knowledge. This causes the fact that numerical analysis must be conducted by an experienced research team, with excessive knowledge of FEM, theories of material laws and their implementations. Huge amount of post-processing data must be carefully revised to prove lack of numerical issues, like: non-physical penetrations, so called "shooting nodes" or hourglass deformations.

If correctly used, LS-DYNA code is a powerful tool in simulation of full-scale tests. Very high quality and quantity compliance with real crash test can be achieved, what gives possibility of a deep insight into the phenomenon. After a successful validation of the model further parametric studies may be conducted, giving a chance of improving the design of analysed structures or studying some extraordinary cases, without spending funds on full scale, experimental crash tests.

2.2 Numerical model of vehicle

Crash tests consists of road safety equipment being tested and a vehicle of specified type. The vehicle's type is an important factor because vehicles differ not only by a weight but also by external geometry, wheel tracks, centre of mass location and so on. During full scale crash tests TB32 as a rule BMW series 5 car was used. Therefore, in order to achieve the best results, numerical model of the same vehicle's brand was used during the validation of a cable road safety barrier numerical model. LS-DYNA's code of BMW, used in this paper, was developed by Transpolis (formerly LIER), the French crash-test house and digital simulation office for road safety equipment. According to the British Standards for numerical simulations [51], [52], [53], [54] to assume the reliability of the vehicle's model a series of validation tests should be performed. These tests are meant to check the overall behaviour of the vehicle's motion and its numerical stability.

Full scale vehicle's picture with a comparison to the corresponding BMW numerical model is displayed in Fig. 4. As it can be seen the vehicle's model has very similar geometry to the full scale car. Moreover, when it comes to the general criteria for the test methods specified in Standards Publication [48], both of the vehicles fulfil the listed requirements. Relevant data concerning numerical model's specification requirements are listed in the Table 3. Vehicle's finite element mesh consists of 20798 shell elements, 1448 beam elements and 970 solids. These numbers of elements correspond to 22668 nodes. Initially, critical time step for calculations using explicit time integration [28] was equal to 6.38E-07 s. In order to increase the critical time step some suspension mesh modifications have been performed. That led to the time step increase and current model's critical time step equals 1.3E-6 s. Preforming numerical simulations of crash tests against cable barriers, discontinuities between car parts provided for contact with wire should be avoided. Thus, nodes of several parts like bumper and grill have their adjacent nodes merged. Tires of the vehicle were modelled with appropriate reinforcement basing on [1], [4], [5], [6].

The vehicle was equipped near the center of gravity with a special finite element that was used to record accelerations and angular velocities in local vehicle coordinate system. This solution made it possible to collect the data necessary to determine ASI and THIV.

Fig. 4 Comparison between BMW car and its numerical model

Table 3. Comparison between numerical vehicles parameters and EN 1317 requirements.

Vehicle specifications	EN 1317 [48]	Numerical model	Is the requirement met?
Total mass, kg	1500 ± 75	1500,5	Yes
Dimensions:			
Front wheel track, m	1,50 ± 0,225	1.49	Yes
Rear wheel track, m	1,50 ± 0,225	1,49	Yes
Wheel radius, m	NA	NA	NA
Wheel base, m	NA	NA	NA
Centre of mass location:			
Longitudinal distance from front axle (CGX)	1,24 ± 0,124	1,24	Yes
Lateral distance from vehicle center line (CGY)	± 0,08	0,001	Yes
Height above ground (CGZ)	0,53 ± 0,053	0,56	Yes

NA – not applicable

2.3 Numerical model of cable barrier system

2.3.1 General description

To analyse the behaviour of the restraint system installed on the horizontal convex curves of the road, a numerical model of the 4-cable barrier has been created (Fig. 5). The barrier's model, including also the soil and the surface on which the vehicle moves, consists of 434710 nodes and 455506 finite elements.

The safety barrier is 81 m long (69 m straight section and two 6 m long terminals). The height of the barrier is approx. 0.78 m. Four wire ropes, each of 19 mm diameter, are mounted in the posts and appropriate distance between the wire ropes is provided by the distance elements. This type of wire rope is commonly used in cable barriers, see [25], [58], [59]. The cables are mounted at height of 0.48, 0.56, 0.64 and 0.72 m above the ground. A steel clamp is additionally attached between the two highest cables. The steel wire ropes are pretensioned and the tensioning element is located between the posts no. 45 and 46. The post spacing is 0.75 m, but due to the placement of the tensioning elements the spacing has to be adjusted to 1.5 m. In the middle section of the barrier, near the impact area, the soil is modelled as cylinders in which the posts are embedded. All the nodes on the cylinder's outer curved surface and on its bottom base surface are fixed. In the other posts simplified method of modelling the ground is used, in which the ground is modelled by fixing all the nodes at the base of the posts (9 cm below the ground surface). This simplified method of ground modelling, in which the ground was modelled only for a part of the barrier, can be found in e.g. [55] where the reliability of such simplification was confirmed. The soil model for a single post is illustrated in the Fig. 6 (similar solution was used in files, which were available on NCAC public library [45]). Other papers that include the description of the soil's material laws usage and a comparison of soil numerical modelling with full scale tests should be also noted, e.g. [19], [66]. The present model does not include additional elements loosely applied to the top of the posts.

The initial time step is equal to 9.15E-07 s due to the shell elements of post. In order to prevent a reduction of the timestep during the calculation, mass scaling was introduced to the model to ensure a minimum timestep of 9.0E-07 s. Trial simulations of the TB32 test were carried out for two cases: without mass scaling and with mass scaling. The most important indicators obtained from tests were compared. For the simulation without mass scaling the results are: ASI = 0.718, THIV = 24.43 km/h, working width = 0.98 m. The calculation time for 1 s of simulation was 59 hours 55 minutes and 18 seconds. In the simulation which included mass scaling the results are as follows: ASI = 0.682, THIV = 24.42 km/h, working width = 0.96 m and for this 1s simulation, the corresponding calculation time amounts to 32 hours and 35 seconds. These two simulations were carried out on computer cluster named Tryton, managed by CI TASK in Gdańsk (Poland) using 192 threads (eight 24-core processors). Because of the differences in the results that are considered

insignificant and the calculation time is reduced by 47%, it was decided to use the mass scaling in all simulations. The maximum nonphysical mass added to the model during all numerical simulations performed for the purpose of this study was equal to 0.525 kg (v = 110 km/h, radius R = 900 m), the minimum mass added during the simulation was equal to 0,001 kg (v = 50 km/h, radius R = 400 m).

A shortened description of the implementation of barrier's elements and parameters is presented in table 4 and table 5. LS-DYNA R.8.1 environment was used in order to perform all the calculations, thus all terms used below are described in detail in the theory documentations [28] [39].

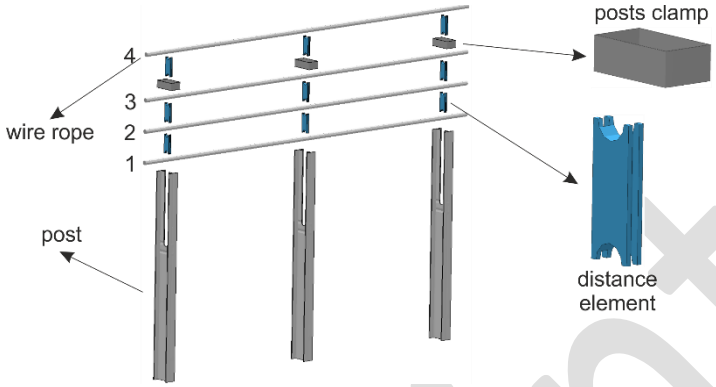

Fig. 5 Components of the cable barrier system

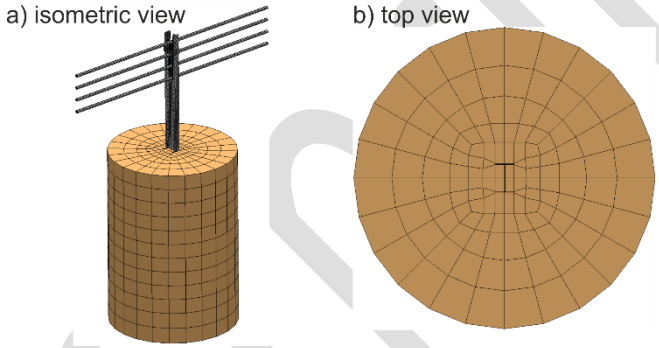

Fig. 6 Soil discretization, a) isometric view, b) top view

Table 4. Short description of the implementation of elements of the model.

Element	**Descriptions**
Wire ropes	Beam elements, Belytschko-Szwer resultant beam formulation (ELFORM_2), *MAT_MOMENT_CURVATURE_BEAM (*MAT_166), material parameters determined based on [56] and [59]
Tensioning elements	Beam elements, discrete beam/cable formulation (ELFORM_6), *MAT_CABLE_DISCRETE_BEAM (*MAT_071), tensile force is 20,4 kN
Posts	Shell elements, Belytschko–Tsay formulation (ELFORM_2), 5 integration points through shell thickness, *MAT_PIECEWISE_LINEAR_PLASTICITY (*MAT_024)
Distance elements	Soil elements, fully integrated selective reduced solid elements (ELFORM_-1), *MAT_RIGID (*MAT_020), On the outside surfaces of plastic elements null shells was applied by using *MAT_NULL material model (*MAT_009), which enable contact with other elements of the numerical model
Clamp	Shell elements, Belytschko–Tsay formulation (ELFORM_2), 5 integration points through shell thickness, *MAT_PIECEWISE_LINEAR_PLASTICITY (*MAT_024)
Soil	Solid elements, constant stress solid element formulation (ELFORM_1) *MAT_SOIL_AND_FOAM (*MAT_005), material parameters taken from [45] null shells with *MAT_NULL material model (*MAT_009) was added on the top and inside surfaces of soil to enable contact between posts and soils
Motion surface	Shell elements, Belytschko–Tsay formulation (ELFORM_2), 2 integration points through shell thickness, *MAT_RIGID (*MAT_020), additionally the *RIGIDWALL_PLANAR card was used

Table 5. Description of the implementation of parameters of the model.

Element	Descriptions
Contact	*CONTACT_AUTOMATIC_GENERAL_INTERIOR for all parts of the model except for the soils and internal null shells of the soil *CONTACT_AUTOMATIC_SURFACE_TO_SURFACE between the internal soil null shells and the posts *CONTACT_INTERIOR only for soil
Hourglass	*CONTROL_HOURGLASS, stiffness form of Type 2 (Flanagan-Belytschko), value of the hourglass coefficient (QH) set to 0.03
Damping	*DAMPING FREQUENCY_RANGE for wire ropes and tensioning elements *DAMPING GLOBAL only at the beginning of the calculations, before the impact *DAMPING_PART_STIFFNESS for wire ropes, tensioning elements, posts, soil

2.3.2 Wire rope model

The most challenging barriers' elements to model are the wire ropes, which have been given a lot of attention during the model preparation. Simulations of the cables have their own specificity due to the additional difficulties in the modelling process. The problem is strongly nonlinear since the geometric nonlinearity along with advanced material laws and high quality contact search algorithms have to be used. The phase of pretensioning of cables, which precedes the actual vehicle's impact, is a kind of problem that does not appear in other types of barriers like i.e. concrete or guiderail steel barriers. A special approach should be used in order to reduce the undesirable numerical effects that accompany this particular method. Based on [59], the wire ropes can be modelled in several ways: as discrete beams; beam and solid; beam and shell (Fig. 7b) or only as beam elements (Fig. 7c). An example of using a beam and shell model can be found in the work [62]. However, in the present work it was decided to use a beam model (the description of the elements is presented in tab. 4). This way of modelling, compared to the model using an additional shell and CNRB elements to simulate contact, reduces significantly the number of nodes and shell finite elements that would be needed to properly describe the contact between the cables and the remaining parts of the model. The material properties of wire ropes were taken from [56], [59]. Authors of these reports, based on their full-scale crash test and simulations, stated that this numerical model of the wire rope behaves correctly and is reliable. In reality the cross-sectional area of wire rope is 154.5 mm^2 (Fig. 7a) and Young's modulus is 116 GPa [56]. However in the numerical model diameter of 19 mm (area 283.5 mm^2) is assumed to enable contact with other parts of the model (Fig. 7c). Therefore, the density was reduced by ratio of cross-sectional area of the rope (154.5 mm^2) to the area of the 19 mm circle (283.5 mm^2) and was set to 4308.5 kg/m^3 (the density of the steel is 7948 kg/m^3) [56]. The Young modulus was reduced in the same manner to the value of 62.882 GPa in order to maintain the time step [56]. Three curves (force-strain, bending moment-bending curvature, torque-rate of twist) defined in material model *MAT_MOMENT_CURVATURE_BEAM were taken from [56] and can be also found in [59] and [62].

Particular attention should be paid to the description of the contact while using only beam elements, as there may be a problem of their penetration through shell or solid elements. In this model the *CONTACT_AUTOMATIC_GENERAL_INTERIOR type of contact was used, which adds the null beams to all the shell meshlines [39]. In order to prevent the occurrence of elements with unwanted hourglass modes the Flanagan-Belytschko stiffness form of hourglass control was used basing on the literature [7] [28] [39].

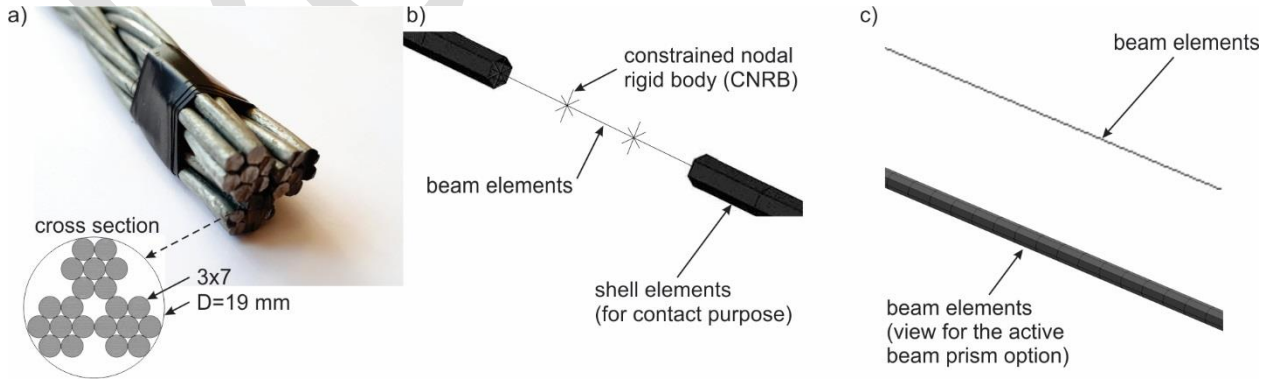

Fig. 7 Wire rope, a) photo, b) beam and shell model, c) beam model

2.4. Simulation procedures: influence of damping and cable tension force

The numerical simulation consists of three main phases: time of free motion of vehicle, the impact phase and the phase in which the vehicle leaves the barrier, see Fig. 8. The first phase (first 0.2 s of simulation) preceding the vehicle impact is very essential. During this phase the proper tension is applied to the wire ropes and at the same time the damping of

the entire system including the barrier and the car is active. A series of simulations was run to test the influence of tensioning phase and the value of global damping on the barrier behaviour and also the influence of global damping on the vehicle behaviour.

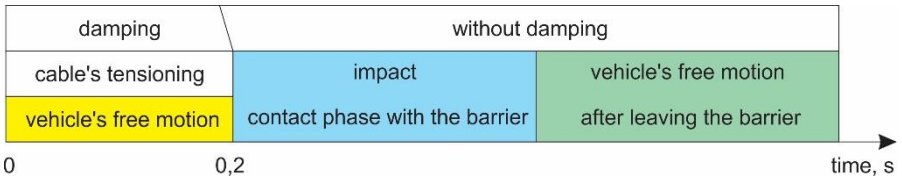

Fig. 8 The phases of crash test numerical simulation

Three cases were studied: no global damping, global damping active (*DAMPING GLOBAL option) on vertical axis with damping constant [39] values either 0.1 or 1.0. The time of active damping was assumed through the initial 0.18s of the simulation and then is reduced to 0 during 0.02s. Thus during the impact phase t≥0.2s the damping is null.

The tension force was imposed through the tensioning elements with *MAT_CABLE_DISCRETE_BEAM [28] assigned. Again three cases of load were studied: instantaneous force of the desired value and two ramping amplitudes: from 0 to the desired value: 0.05s and 0.1s

The above analyses let to the conclusion that instantaneous force yields undesired influence on the force in cables. On the other hand, ramping the value of the force guarantees appropriate values of that force. In addition, the influence of damping on forces in cables in cables's tensioning phase was observed to be negligible.

However, damping has visible effect when vehicle's motion during approach to barrier is considered. As a result of 1s free motion of the car, it was found that the value of ASI index shows unstable oscillations (Fig. 9a) and its peak value is high comparing to the values that are observed during the actual impact phase. Thus null damping was not considered. With damping coefficient values equal to 0.1 the oscillations of ASI are controlled (Fig. 9b) and once the damping dies out (t≥0.2s) the resulting value of ASI remains stable and is small in comparison with that calculated during impact. The value 1.0 of the global damping constant (Fig. 9c) yields larger deceleration of the vehicle during the phase of active damping (yellow area in Fig 9). Consequently, ASI value grows. Further increase of the damping value is meaningless, because as a result of this the vehicle is subject to progressive decelerations and for large damping values, the vehicle is stopped immediately after the beginning of the calculation and due to this very high ASI values are obtained. Therefore, higher values of damping are not considered.

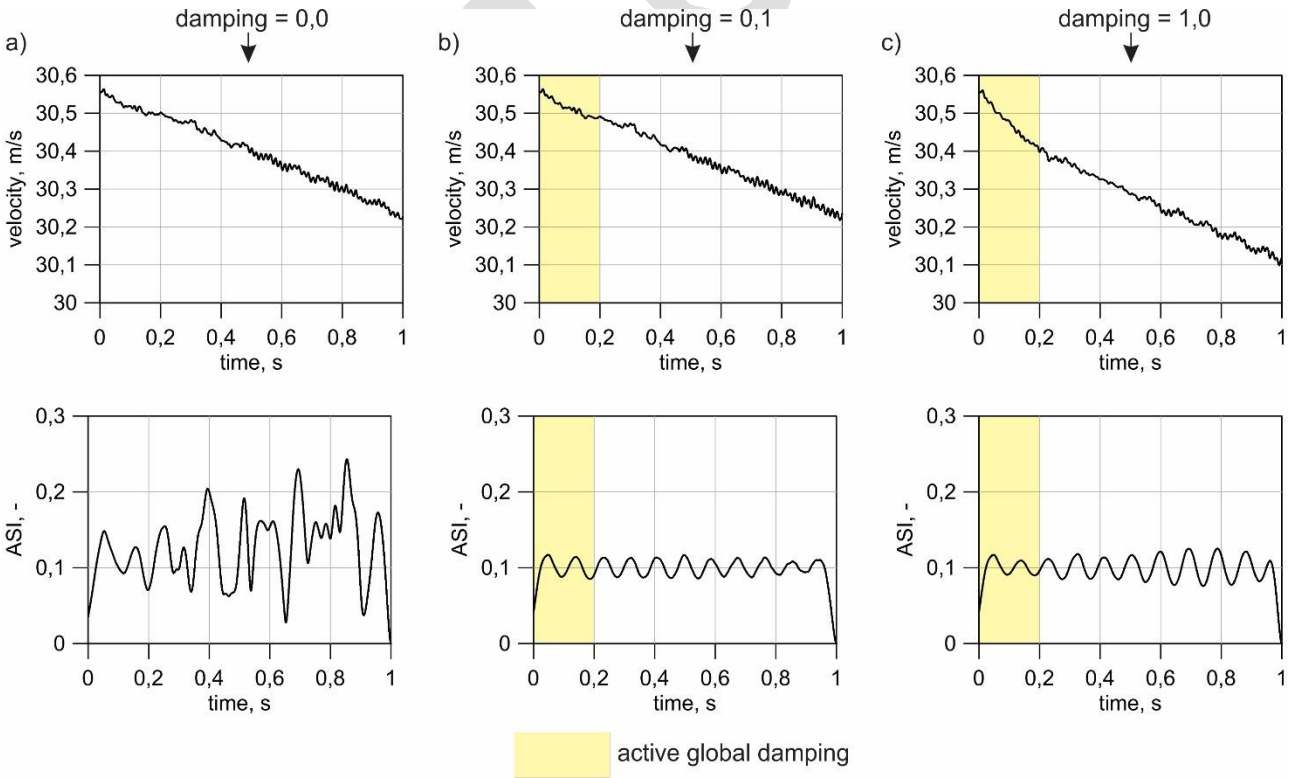

Fig. 9 Free motion vehicle driving test for 1 second - the graphs of velocity (top) and ASI (bottom) for the following cases: a) no global damping, b) global damping = 0,1, c) global damping = 1,0

Base on the above analysis the damping coefficient value was set to 0.1. The ramping phase for the force was set to 0.05s which is portrayed in Fig. 14 (right side). The influence of these settings on the results is to be discussed in paragraph 4 and Fig. 12.

3 Account of the series of the numerical simulation

The study considers all the cases listed in table 2. Thus, a total of 23 simulations was performed for 5 different horizontal curvatures (100 m; 200 m; 400 m; 600 m; 900 m) and also for the straight section of the barrier and for 5 different velocities. The impact speed of 50 km/h corresponds to the speed limit in built-up areas in Poland during the day, between 05:00-23:00. Velocity 70 km/h is a popular speed limit on Polish roads in no built-up area whereas 90 km/h is the maximum speed on single carriageways. 110 km/h corresponds to the speed in the standard TB32 crash test [49] and the velocity 140 km/h is the speed limit on motorways in Poland. In all the simulations, a 1500 kg BMW car impacted the barrier at 20° angle to the tangent of the curve. This values are associated with standard TB32 crash test (110 km/h, 20°, 1500 kg) [49], but in these tests the impact velocity and the radius of the barrier curve are modified. In all the considered cases, the cable barrier was installed on a horizontal plane. The impact location was set in 1/3 length of the barrier, 27 m from the beginning of the barrier. General view of the analysed variants is presented in Fig. 10. An example of the barrier's dimensions in one test (radius R = 100 m) is shown in Fig. 11.

The simulations were performed in order to assess the contribution of the impact velocities and radii of the arcs on the overall performance parameters and impact severity indices of the system. Furthermore, in depth analysis of the axial forces during the simulation in the lowest cable was conducted for a single case. It concerns the TB32 crash test with cable barrier of radius equal to 400 m.

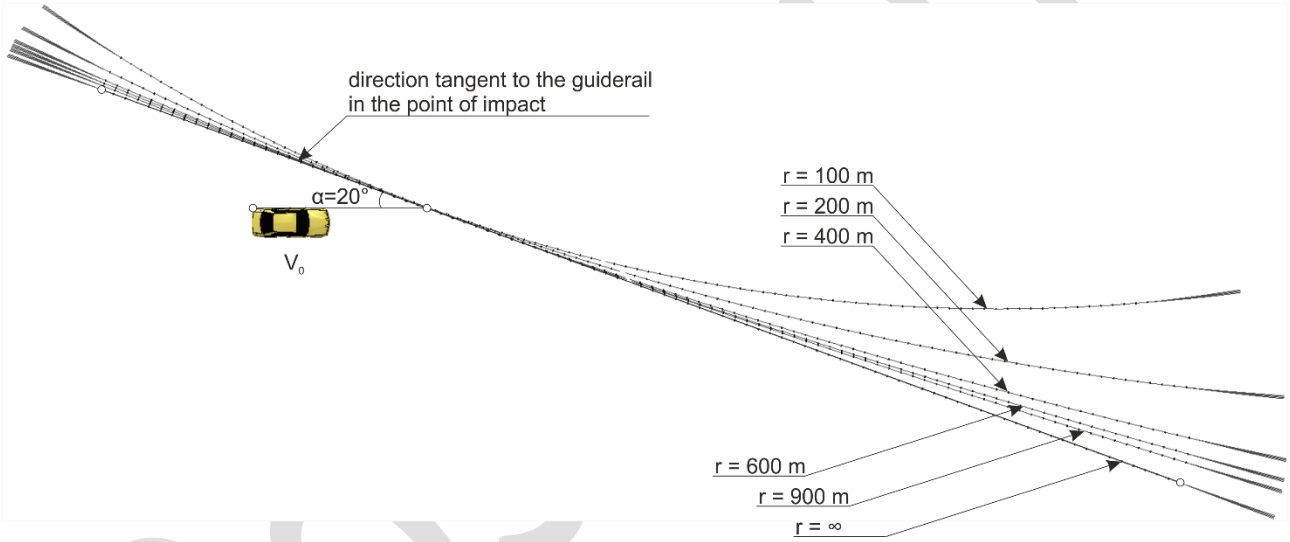

Fig. 10 Overall view of analysed variants

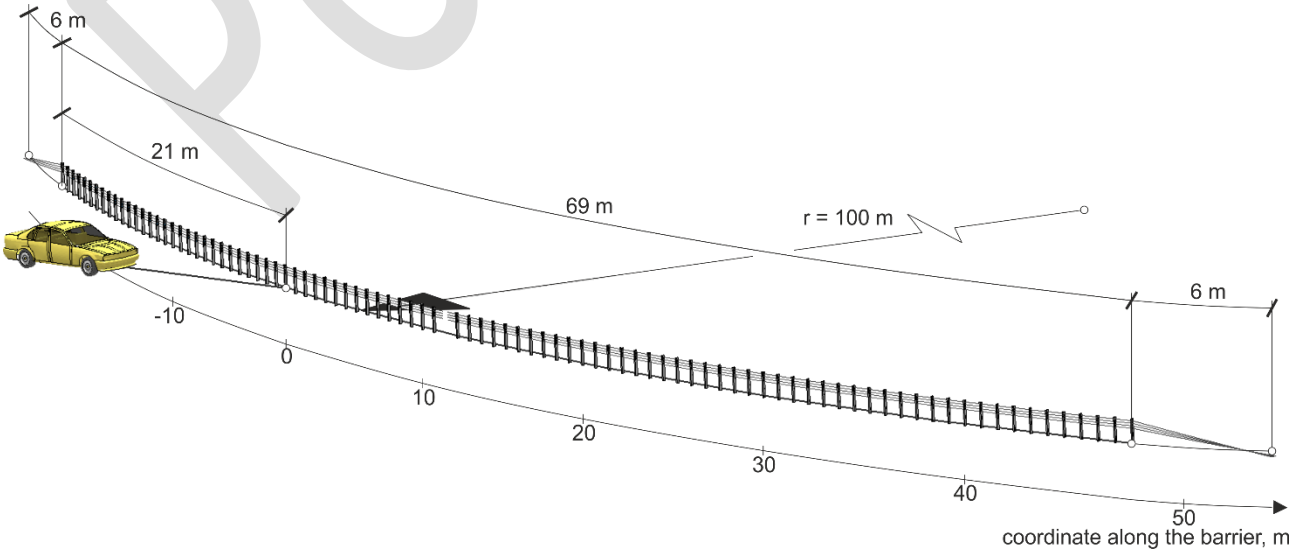

Fig. 11 Dimensions of the analysed barrier for the radius R = 100 m

4 Results of the numerical simulations

Table 6 displays the key indices of the road restraint system i.e. ASI, THIV and the working width. Fig. 12 portrays their graphical interpretation. In every test the barrier contained the vehicle and properly redirected the car back on the traffic lane. Time during which the car was in contact with the barrier was approx. 0.5 s. The impact resulted in bending of the posts towards the ground allowing the cables to detach from the posts. After the impact, the cables deformed car's chassis locally just above the wheels which enabled keeping the cables at the height guarantying the containment and appropriate redirection of the car. The highest wire rope (no. 4) slipped over the hood of the vehicle and then stopped at the level of half of the height of the door's windows. As a result of cables' detaching, the distance elements along with steel clamps were scattered into the air, see e.g. Fig. 13. In some tests, when determining the working width, the translation of the highest wire rope (no. 4 in Fig. 5) was omitted. The reason for this was its significant displacement after impact, which was assumed unreliable as the value of the working width. In this particular case, the depth of car's penetration into the barrier was considered more adequate.

Table 6. Results of the crash test simulations.

Radius, m	Velocity, km/h	ASI, -	THIV, km/h	W_N[1], m	nomenclature
∞ (straight barrier)	90	0,57	24,8	0,74	Rinf_90
	110	0,68	24,4	0,96	Rinf_110
	140	0,94	26,5	1,43	Rinf_140
900	90	0,51	22,1	0,72	R900_90
	110	0,65	24,2	0,94	R900_110
	140	0,90	26,6	1,37	R900_140
600	70	0,51	26,1	0,58	R600_70
	90	0,56	23,7	0,77	R600_90
	110	0,70	24,4	0,95	R600_110
	140	0,93	25,5	1,40	R600_140
400	50	0,39	21,6	0,37	R400_50
	70	0,50	22,3	0,46	R400_70
	90	0,60	22,9	0,75	R400_90
	110	0,66	24,5	0,91	R400_110
	140	0,88	24,8	1,42	R400_140
200	50	0,42	23,6	0,42	R200_50
	70	0,49	24,3	0,54	R200_70
	90	0,58	23,4	0,75	R200_90
	110	0,65	24,4	1,00	R200_110
100	50	0,48	26,5	0,43	R100_50
	70	0,45	24,3	0,56	R100_70
	90	0,52	26,0	0,76	R100_90
	110	0,72	27,6	0,89	R100_110

[1] the highest rope not included, justification in the text

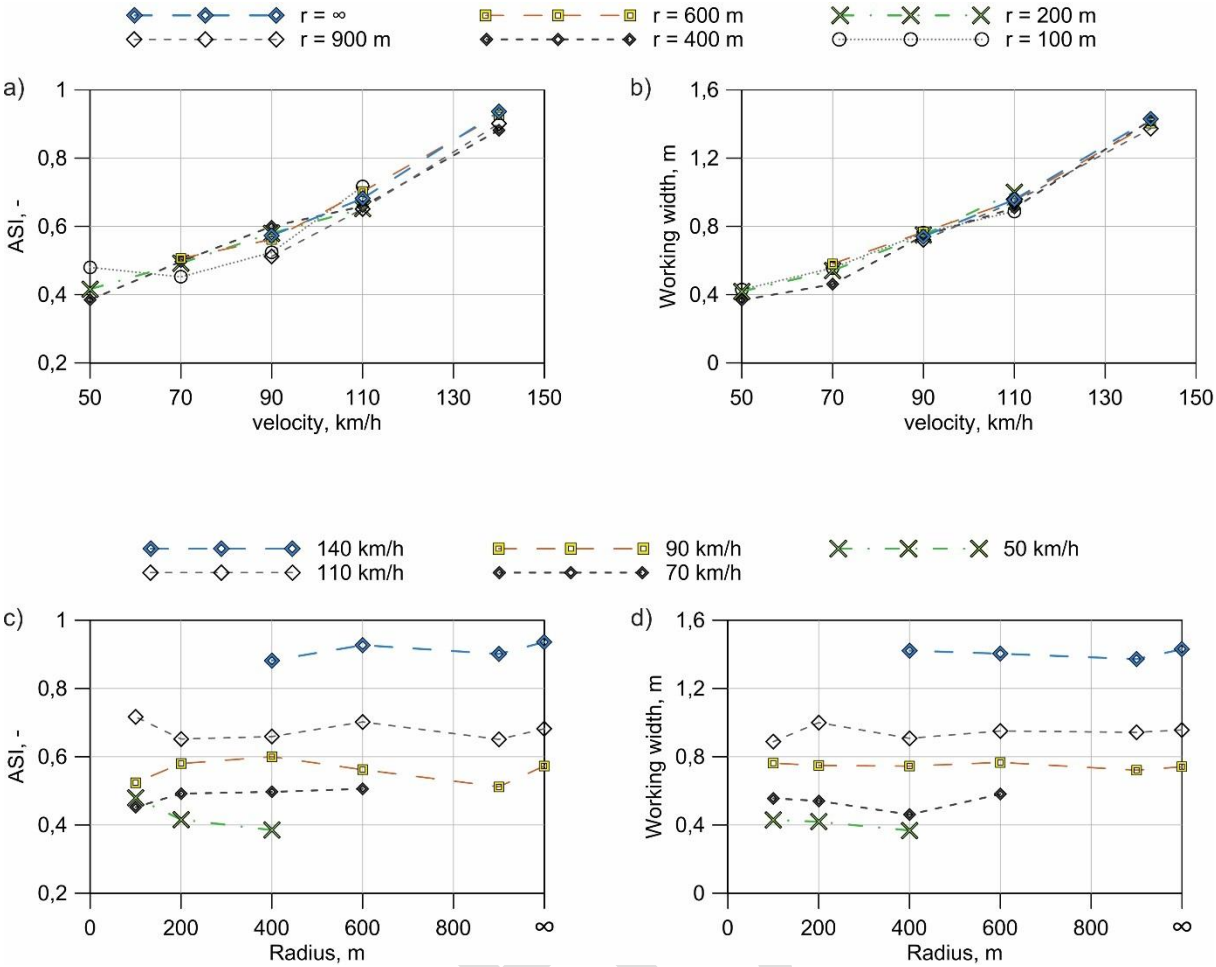

Fig. 12. Results, a) ASI depending on velocity for different radius, b) Working width depending on velocity for different radius, c) ASI depending on radius for different velocities, d) Working width depending on radius for different velocities

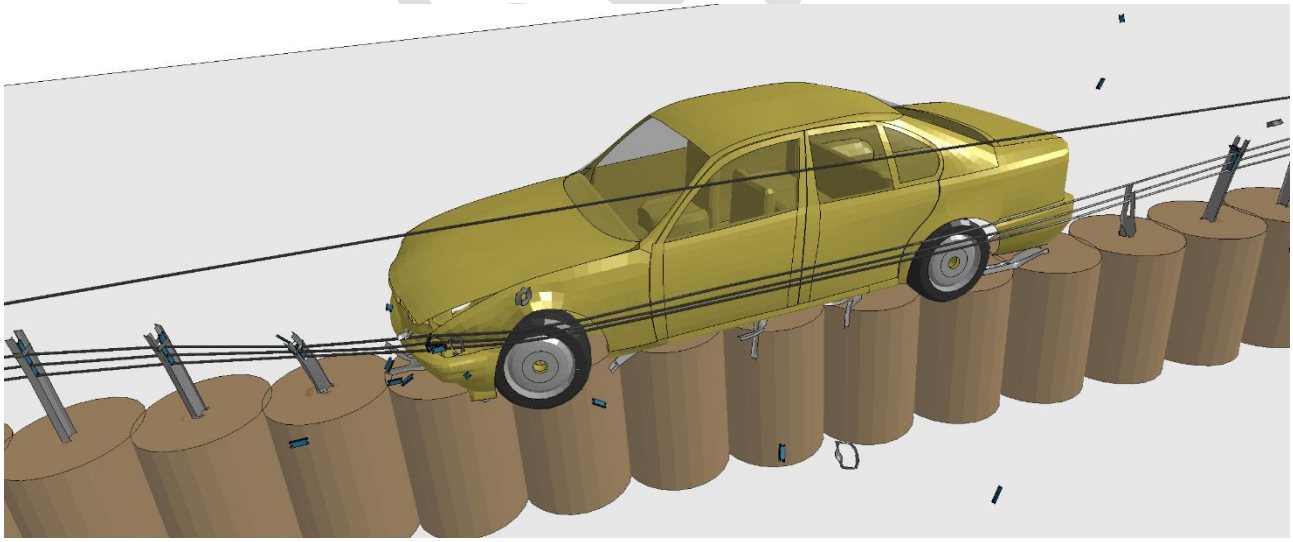

Fig. 13. The view during impact of the TB32 crash test (test Rinf_110)

The tensioning phase of the wire ropes in numerical environment leads to interesting results regarding the axial forces in the wire rope. Results presented in Fig. 14, Fig. 15, Fig. 16 refer to the TB32 crash test with the radius of 400 m. Fig. 14 depicts the curves of axial forces in the rope no.1 (see Fig. 5) versus the coordinate along the barrier for given moments of time in simulation. The location of the tensioning element is marked with grey dashed line in the centre of the picture. The small graph on the right shows the variation of the force in the tensioning element in time. Moreover, the time instances corresponding to the remaining curves in the figure are marked with blue dots. It can be noticed that with the increase of time (and the value of the tension force) the shape of the line changes from wavy form to the almost straight. At time 0.19 s, just before the impact, the difference between extreme force values (in straight horizontal section of the wire rope) was approx. 0.249 kN. Considering the deviatoric post displacement, shown in Fig. 14 (left side) it can be noticed that the deformation of the post progresses along the direction of the wires and results in the reduction of the force value.

Fig. 15 displays the top views of the vehicle's impact against the safety system and the curves of the axial force. It is noted that the rapid changes of the tension force appear in the collision point. Then, the force is transmitted through the entire length of the rope. As the vehicle proceeds, the value of the axial force rises to its extreme value (for the lowest rope) equal to 76.38 kN at time = 0.32s. Then the car is redirected and pushed in the opposite direction, as seen in Fig. 16. Though the residual forces in time = 1.0 s are not the final ones it can be noticed that the values of the forces tend toward the initial pre-tensioned value, equal to 20.4 kN. The locations of 11 detached posts are marked with dark green symbols.

During the simulation, the posts deform exerting the forces on the ground. Therefore, it is justifiable to study the results of that deformation from the viewpoint of the surrounding soil. The effective stresses based on Huber-Mises-Hencky hypothesis are plotted in Fig. 17 in three adjacent posts located nearby the impact point. Two separate time steps are displayed to distinguish the moment of impact and the stresses in time = 1.0 s.

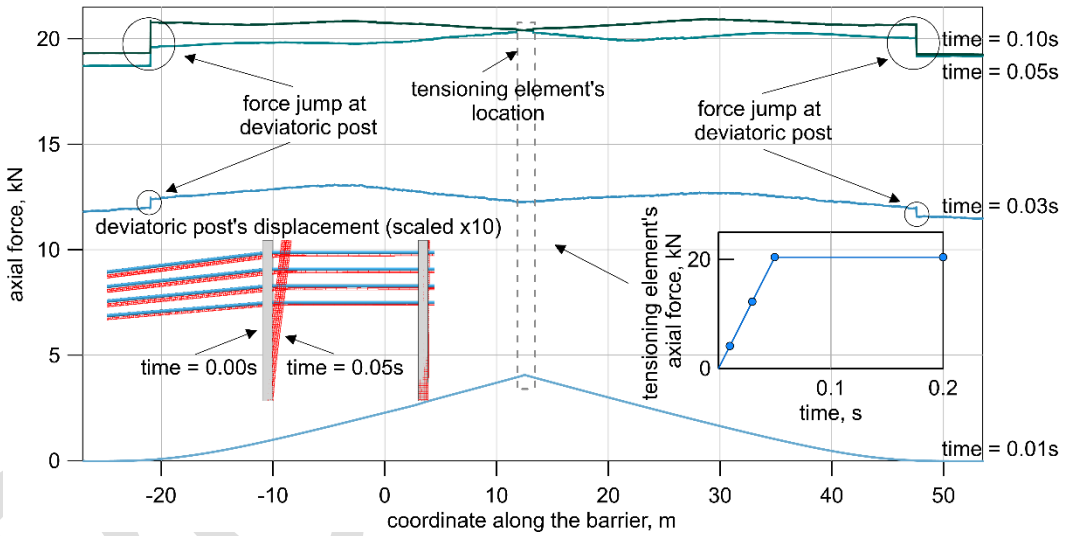

Fig. 14 Axial forces in the wire rope no. 1 during tensioning

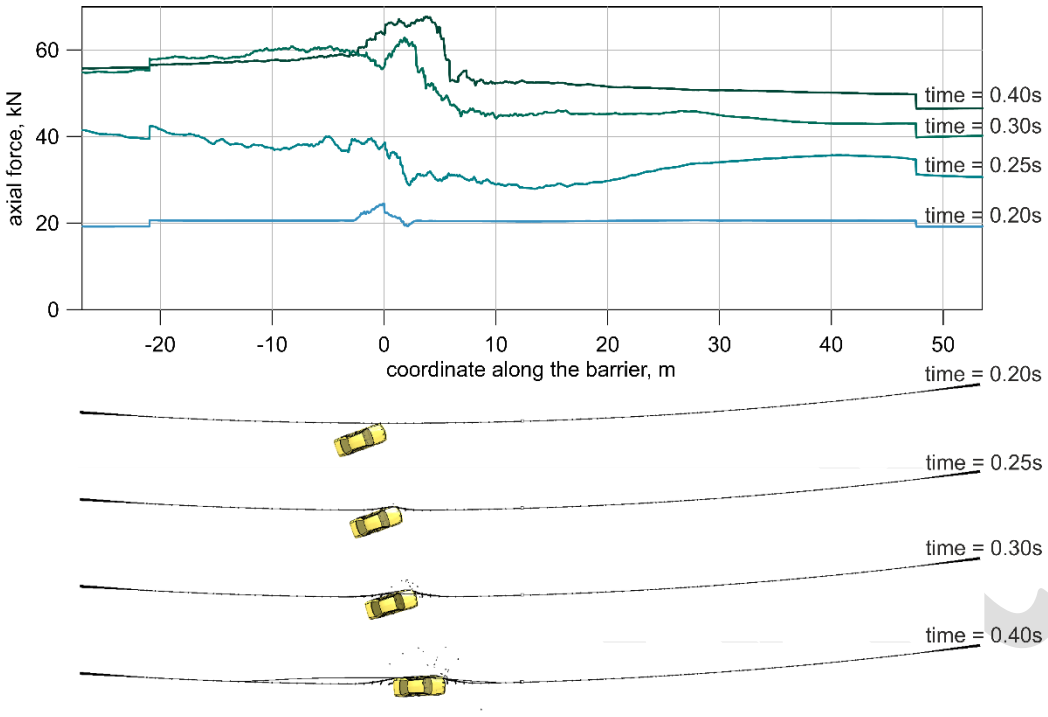

Fig. 15 Axial forces in the wire rope no. 1 and top-view snapshot during impact at selected time points

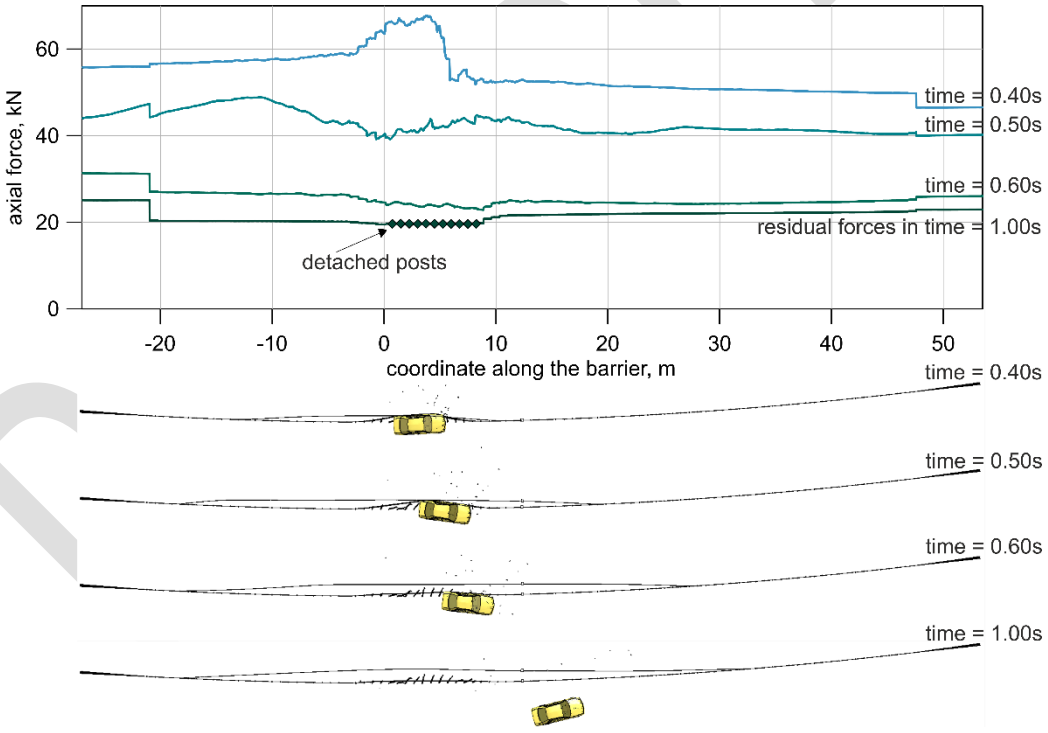

Fig. 16 Axial forces in the wire rope no. 1 and top-view snapshot during impact and after leaving the barrier by vehicle at selected time points

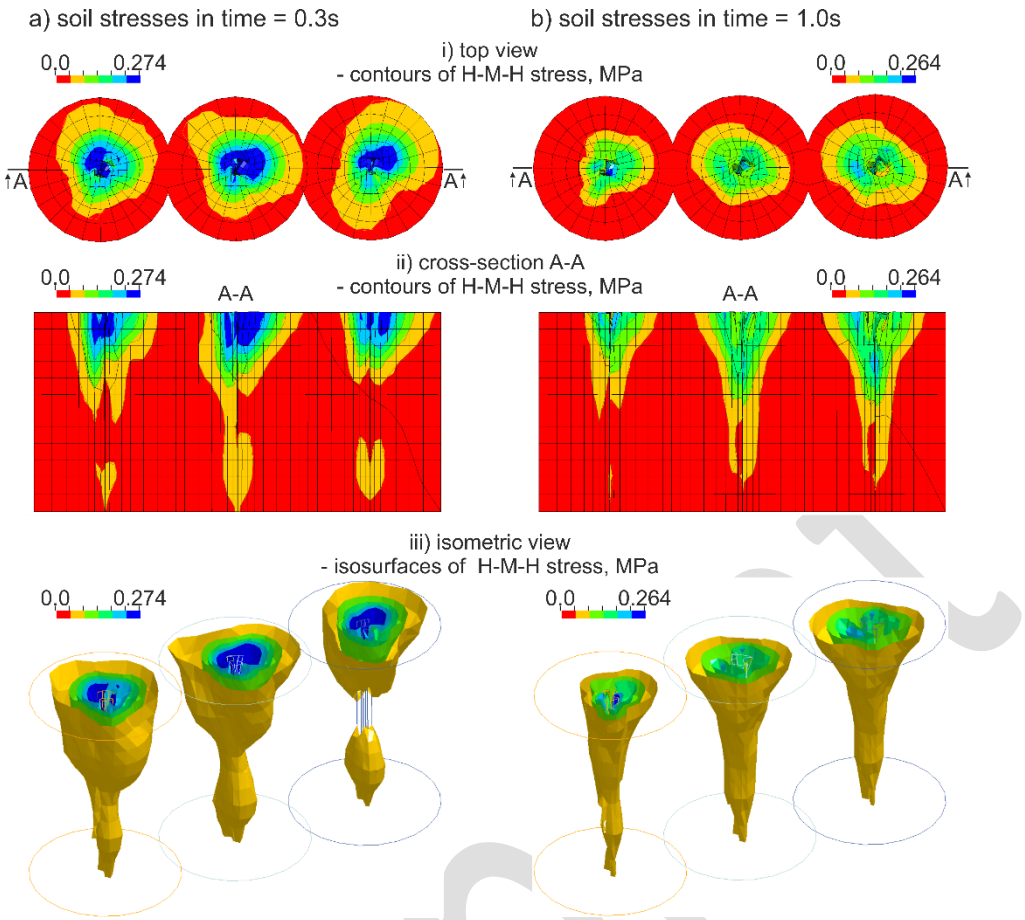

Fig. 17 Huber-Mises-Hencky stresses in soil

Analysis of the simulation data allows to draw the conclusion that when the initial velocity increases (equivalently initial kinetic energy), the values of ASI and working width also increase. Consequently, the number of damaged posts and time of contact between car and the barrier rises as well. The visibly increasing trend of the analysed indices is observed (Fig. 12). An important effect of the study is value of ASI<1,0 and THIV<33 km/h that indicate high safety of car passengers. In case of the analysed barrier, its placement along the horizontal arc does not influence negatively on the obtained values even for relatively small radius R = 100 m. The results obtained for given velocities are similar and do not vary much with the radius. It should be stressed that the analysed barrier has posts at close distance i.e. every 75 cm and the barrier is capable of containing the bus. The latter results are presented in [62]. In case of the barriers placed along the road's curve, such a dense placement of the posts mitigates the negative effect on the change of line's curvature into secant line which is responsible for the drop of the initial tension in line. This is confirmed by guidelines of some producers and this conclusion can be found in report [25].

Summarizing the obtained results it can be concluded that the value of the radius has smaller influence on the severity levels than the impact velocity. Therefore, it is possible to use such barriers along road arc with the post placed at most at every 75 cm.

5 Conclusions

Relatively larger number of accidents have been reported on road horizontal curves. This elements of road infrastructure, in the last ten years, have had approx. 10% of all road accidents representing approx. 14% of all fatalities on Polish roads. The data shows that in the case of accidents on horizontal curves approx. 45% of the fatalities happened as a result of crashing into roadside obstacles such as trees or signs. This shows that horizontal curves require road safety equipment, and specifically, safety barriers. Key to this is using the right equipment with the right parameters.

The use of numerical simulations for performing virtual crash tests is becoming more and more common. Thanks to simulations, it is possible to follow the dynamic phenomena occurring during the impact and investigate many details that are inaccessible by any other method. The numerical modelling procedures for the cable barriers are complex and should be further developed. Some general concepts for steel wire rope barriers modelling was presented. The parameters of the system's numerical model elements were summarized and briefly described. The tests of the barrier were conducted to analyse the influence of the convex curve radius and the initial vehicle conditions on the impact severity indexes and performance parameters. Thus, according to the European Standards [49], the ASI and THIV parameters qualified the 4-cable guardrail road safety system to the A class for all analysed types of horizontal convex curves with radius variating

from R=100 m till straight line. It means that, basing on this results, this type of barrier may be considered relatively safe for the occupants of the car. As suspected, the vehicle's velocity during impact pays crucial role due to the fact that the kinetic energy rises squared. The radius of the barrier's curve doesn't significantly influence the value of working width. However, when analysing these types of issues, it is important to carefully analyse the input model code and the results. A feature of such highly non-linear problems is that the results may vary depending on many parameters, e.g. soil material laws, cable pretension force, the dynamic and static friction. Thus, all the assumptions shall be described in detail.

This work was supported by the National Centre for Research and Development (NCBiR) and General Director for National Roads and Motorways (GDDKiA) under the research project "Road Safety Equipment" (contract number DZP/RID-I-67/13/NCBR/2016). The BWM vehicle model was developed by Transpolis (formerly LIER), the French crash-test house and digital simulation office for road safety equipment. Calculations have been carried out at the Academic Computer Centre in Gdańsk, Gdańsk University of Technology.

References

[1] AASHTO, Highway Safety Manual. Washington: American Association of State Highway and Transportation Officials, 2010.
[2] M. Abdel-Aty, A.E. Radwan: Modeling traffic accident occurrence and involvement, Accid. Anal. Prev. 32 (2000) 633–42.
[3] P. Baranowski, J. Małachowski, J. Janiszewski, J. Weekezer, Materials and Design, 96, 68-79, (2016)
[4] P. Baranowski, J. Małachowski, L. Mazurkiewicz, International Journal of Mechanical Sciences, 106, 346-356, (2016)
[5] P. Baranowski, J. Janiszewski, J. Małachowski, Journal of Theoretical and Applied Mechanics, 55, 727-739, (2017)
[6] P. Baranowski, J. Małachowski, Bulletin of the Polish Academy of Sciences, 63, 867-878, (2015)
[7] T. Belytschko, W. K. Liu, B. Moran, Nonlinear Finite Elements for Continua and Structures, (2000)
[8] W. Borkowski, Z. Hryciów, P. Rybak, J. Wysocki: Numerical simulation of the standard TB11 and TB32 tests for a concrete safety barrier, Journal of KONES Powertrain and Transport, Vol. 17, No. 4, 2010, s. 63-71
[9] D. Bruski, W. Witkowski, Numerical studies on the influence of selected construction features and road conditions on the performance of road cable barriers, MATEC Web of Conferences 231, 01003, GAMBIT 2018 (2018).
[10] D. Bruski, S. Burzyński, J. Chróścielewski, Ł. Pachocki, W. Witkowski, On the validation of the LS-DYNA Geo Metro numerical model, MATEC Web of Conferences 262, 10001, KRYNICA 2018, (2019).
[11] P. Buddhavarapu, A. Banerjee and J. A. Prozzi: Influence of pavement condition on horizontal curve safety. Accident Analysis & Prevention, 52:9 – 18, 2013.
[12] M. Budzynski, K. Jamroz, L. Jelinski, and M. Antoniuk, "Why are Trees Still Such a Major Hazard to Drivers in Poland?," W: 6th Transport Research Arena (TRA), 2016, ELSEVIER SCIENCE BV
[13] M. Budzyński, D. Bruski, Assessing vehicle restraint systems on horizontal curves, MATEC Web of Conferences 231, 01004, GAMBIT 2018 (2018).
[14] S. Cafiso, A. Di Graziano, G. Di Silvestro, G. La Cava, B. Persaud: Development of comprehensive accident models for two-lane rural highways using exposure, geometry, consistency and context variables, Accid. Anal. Prev. 42 (2010) 1072–9.
[15] S. G. Charlton: The role of attention in horizontal curves: A comparison of advance warning, delineation, and road marking treatments. Accident Analysis & Prevention, 39(5):873 - 885, 2007.
[16] T. Esposito, R. Mauro, F. Russo-1, and G. Dell'Acqua: Speed prediction models for sustainable road safety management. Procedia - Social and Behavioral Sciences, 20:568 – 576, 2011. The State of the Art in the European Quantitative Oriented Transportation and Logistics Research, 4th Euro Working Group on Transportation & 26th Mini Euro Conference & 1st European Scientific Conference on Air Transport.
[17] EuroRAP, Road protection score (RPS) method and pilot results, 2002.
[18] H. Fang, Q. Wang, D. Weggel, Crash analysis and evaluation of cable median barriers on sloped medians using an efficient finite element model, AiES, 82 pp. 1-13 (2015)
[19] E. L. Fasanella, K. E. Jackson, S. Kellas, Soft Soil Impact Testing and Simulation of Aerospace Structures, 10th International LS-DYNA Users Conference, (2008)
[20] A. Fernandes, J. Neves, An approach to accidents modeling based on compounds road environments., Accid. Anal. Prev. 53 (2013) 39–45.
[21] R. Fuller: Towards a general theory of driver behaviour., Accid. Anal. Prev. 37 pp. 461–72 (2005). doi:10.1016/j.aap.2004.11.003
[22] Federal Highway Administration, Accident modification factors, United States Dep. Transp. (2005).
[23] M. Garnowski, H. Manner: On factors related to car accidents on German Autobahn connectors, Accid. Anal. Prev. 43 (2011) 1864–71.
[24] GDDKiA, Wytyczne stos. drogowych barier ochronnych na drogach krajowych (2010)
[25] Guidance for the Selection, Use, and Maintenance of Cable Barrier Systems, NCHRP REPORT 711, (2012).
[26] M. Gutowski, E. Palta, H. Fang: Crash analysis and evaluation of vehicular impacts on W-beam guardrails placed behind curbs using finite element simulations, Advances in Engineering Software, 114, pp. 85–97 (2017).

[27] M. Gutowski, E. Palta, H. Fang: Crash analysis and evaluation of vehicular impacts on W-beam guardrails placed on sloped medians using finite element simulations, Advances in Engineering Software, 112, pp. 88-100 (2017).
[28] J. Hallquist, *Ls-Dyna Theory Manual* (2006).
[29] J. M. Holdridge, V. N. Shankar, and G. F. Ulfarsson, "The crash severity impacts of fixed roadside objects," *J. Safety Res.*, vol. 36, no. 2, pp. 139–147, Jan. 2005.
[30] S.G. Ison, M. Quddus, C. Wang: Predicting accident frequency at their severity levels and its application in site ranking using a two-stage mixed multivariate model, Accid. Anal. Prev. 43 (2011) 1979–90.
[31] J.N. Ivan, P.E. Garder, Z. Deng, C. Zhang: The effect of segment characteristics on the severity of head-on crashes on two-lane rural highways, University of Connecticut, University of Maine, 2006.
[32] A. Jacob, R. Dhanya, and M.V.L.R. Anjaneyulu: Geometric design consistency of multiple horizontal curves on two lane rural highways. Procedia - Social and Behavioral Sciences, 104:1068 – 1077, 2013. 2nd Conference of Transportation Research Group of India (2nd CTRG).
[33] C. Jurewicz and R. Excel: Application of a crash-predictive risk assessment model to prioritise road safety investment in Australia. Transportation Research Procedia, 14:2101 – 2110, 2016. Transport Research Arena
[34] H. Karim, M. Magnusson, M. Wiklund, Assessment of Injury Rates Associated with Road Barrier Collision. Procedia – Social and Behavioral Sciences, no. 48. (2012)
[35] W. Kustra, K. Jamroz, M.Budzyński: Safety PL - a support tool for Road Safety Impact Assessment, W: 6th Transport Research Arena (TRA), 2016, ELSEVIER SCIENCE BV
[36] W. Kustra, L. Michalski: Tools for road infrastructure safety management in Poland. MATEC Web of Conferences 122, 02008 (2017). GAMBIT 2017
[37] P. Larsson, S.W.A. Dekker, C. Tingvall, The need for a systems theory approach to road safety, Saf. Sci. 48 pp. 1167–1174 (2010). doi:10.1016/j.ssci.2009.10.006
[38] J. Lee, F. Mannering: Impact of roadside features on the frequency and severity of run-off-roadway accidents: an empirical analysis, Accid. Anal. Prev. 34 (2002) 149–61.
[39] LS-DYNA keyword user's manual, LIVERMORE SOFTWARE TECHNOLOGY CORPORATION (LSTC), California, USA (2015)
[40] M. Klasztorny, K. Zielonka, D. B. Nycz, P. Posuniak, Experimental verification of simulation of TB32 crash test for SP-05/2 road safety barier on horizontal arc, JCEEA, Vol. XXXIV, 64 (2/I/17) pp. 107-118 (2017)
[41] S. Mondal, Y. Lucet, and W. Hare: Optimizing horizontal alignment of roads in a specified corridor. Computers & Operations Research, 64:130 - 138, 2015.
[42] L. Mikołajków, *Drogowe bariery ochronne*. WKŁ, Warszawa, (1983) (in Polish)
[43] L. Mikołajków, Drogowe bariery ochronne linowe, Mag. Autostr., 11 pp. 34-41 (2006) (in Polish)
[44] R. P. Nasution, R. A. Siregar, K. Fuad, A. H. Adom: The effect of ASI (Acceleration Severity Index) to different crash velocities, Proceedings of International Conference on Applications and Design in Mechanical Engineering (ICADME), Malaysia, 11-13 October 2009, pp. 1-6.
[45] National Crash Analysis Center, http://www.ncac.gwu.edu/vml/models.html, date of access 10.03.2016.
[46] NCHRP Report 500 Volume 7: A guide for reducing collisions on horizontal curves, Transportation Research Board, Washington, D.C., 2003
[47] S. Othman, R. Thomson and G. Lanner: Safety analysis of horizontal curves using real traffic data. Journal of transportation engineering, 140(4):04014005, 2013
[48] PN-EN 1317-1:2010. *Road restraint systems* – part 1: Terminology and general criteria for test methods
[49] PN-EN 1317-2:2010. *Road restraint systems* – part 2: Performance classes, impact test acceptance criteria and test methods for safety barriers including vehicle parapets
[50] PN-EN 1317-5+A2:2012. *Road restraint systems* – part 5: Product requirements and evaluation of conformity for vehicle restraint system
[51] PD CEN/TR 16303-1:2012. Road Restraint Systems – Guidelines for computational mechanics of crash testing against vehicle restraint system. Part 1: Common reference information and reporting (2012)
[52] PD CEN/TR 16303-2:2012. Road Restraint Systems – Guidelines for computational mechanics of crash testing against vehicle restraint system. Part 2: Vehicle Modelling and Verification (2012)
[53] PD CEN/TR 16303-3:2012. Road Restraint Systems – Guidelines for computational mechanics of crash testing against vehicle restraint system. Part 3: Test Item modelling and Verification (2012)
[54] PD CEN/TR 16303-4:2012. Road Restraint Systems – Guidelines for computational mechanics of crash testing against vehicle restraint system. Part 4: Validation Procedures 2012.
[55] G. Qian, M. Massenzio, M.Ichchou: Development of a W-beam Guardrail Crashing Model by considering the Deformations of Components, ICMCE '16, December 14-17, 2016, Venice, Italy (2016).
[56] J. Reid, K. Lechtenberg, C. Stolle, *Development of Advanced Finite Element Material Models for Cable Barrier Wire Rope* (2010)
[57] Z. Ren, M. Vesenjak: Computational and experimental crash analysis of the road safety barrier, Engineering Failure Analysis, 12, 2005, pp. 963-973.
[58] C.S. Stolle, J.D. Reid, Development of a wire rope model for cable guardrail simulation, International Journal of Crashworthiness, Vol. 16, No. 3, pp. 331-341 (2011)
[59] C.S. Stolle, J. Reid, Modeling Wire Rope Used in Cable Barrier Systems, 11th International LS-DYNA Users Conference, pp. 1-10 (2010)

[60] Technical conditions that should be met by public roads and their location, MIB Warsaw 2016
[61] T. Teng, C. Liang, T. Tran: Development and validation of finite element model for road safety barrier impact tests, Simulation: Transactions of the Society for Modeling and Simulation International, Vol. 92 issue 6, 2016, pp. 565-578
[62] K. Wilde, D. Bruski, S. Burzyński, J. Chróścielewski, W. Witkowski, Numerical crash analysis of the cable barrier, Mathematical and Numerical Aspects of Dynamical System Analysis, http://repozytorium.p.lodz.pl/handle/11652/1760, date of access 10.03.2016, pp. 555-566 (2017),
[63] K. Wilde, S. Burzyński, D. Bruski, J. Chróścielewski, W. Witkowski, TB11 test for short w-beam road barier, 11th European LS-DYNA Conference, Salzburg, DYNAmore GmbH, 2017, s.1-10
[64] K. Wilde, K. Jamroz, D. Bruski, M. Budzyński, S. Burzyński, J. Chróścielewski, W. Witkowski, Curb-to-barrier face distance variation in a TB51 bridge barrier crash test simulation, AoCE, 63, iss. 2 pp. 187-199 (2017)
[65] K. Wilde, K. Jamroz, M. Budzyński, D. Bruski, S. Burzyński, J. Chróścielewski, Ł. Pachocki, W. Witkowski, Numerical simulations of curved road steel barier (in Polish), JCEEA, Vol. XXXIV, 64 (3/I/17) pp. 535-546 (2017)
[66] W. Wu, R. Thomson, A study of the interaction between a guardrail post and soil during quasi-static and dynamic loading, IJoIE, 34, 883-898, (2007)
[67] G. Yannis, A. Dragomanovits, A. Laiou, T. Richter, S. Ruhl, F. La Torre: Domenichini L., Graham D., Karathodorou N., and Li H. Use of accident prediction models in road safety management – an international inquiry. Transportation Research Procedia, 14:4257 – 4266, 2016. Transport Research Arena.
[68] Y. Zou and A. P. Tarko, "Barrier-relevant crash modification factors and average costs of crashes on arterial roads in Indiana," *Accid. Anal. Prev.*, vol. 111, pp. 71–85, 2018.